Research Article

Evaluation of High Temperature Dry Sliding Wear Behaviour of Thermal Sprayed and Microwave Fused WC12Co and CeO_2 Modified WC12Co Composite Coatings

Pradeep Dyavappanakoppalu Govindaswamy*, Venkatesh Channarayapattana Venkataramaiah and Nithin Hiriyuru Shivegowda
Department of Mechanical Engineering, Malnad College of Engineering, Hassan, Visvesvaraya Technological University, Belagavi, Karnataka, India

Subba Rao Medabalimi
Department of Mechanical Engineering, National Institute of Technology Karnataka, Surathkal, Karnataka, India

* Corresponding author. E-mail: pradeepdgmce@gmail.com DOI: 10.14416/j.asep.2022.03.007
Received: 5 January 2022; Revised: 5 February 2022; Accepted: 4 March 2022; Published online: 29 March 2022

Abstract
Thermal spray methods are used to increase the wear resistance of working surfaces. Microwave post-treatment is the advanced approach for enhancing the properties of thermal spray coatings. The current investigation focuses on the wear behavior of HVOF-sprayed and microwave-treated coatings. The WC12Co and CeO_2 modified WC12Co composite coatings were successfully deposited on AISI4140 steel using the HVOF thermal spray technique. The coatings were tested in both as-sprayed and microwave post-treatment conditions. The dry sliding wear tests were carried out at temperatures of RT, 200, 400, and 600 °C with various loads. Vickers hardness tester, Scanning Electron Microscopy (SEM), and X-ray diffraction (XRD) equipments were used to investigate the microhardness, microstructure, and phases of coatings, respectively. In both compositions, the microwave-fused coating had a fine homogeneous structure and higher hardness than the as-sprayed depositions. For typical loads of 20 N and 40 N for both compositions, the friction coefficient decreased with increasing temperature in the as-sprayed and fused coatings. At all conditions, the microwave fused coating outperforms the as-sprayed coating in terms of wear resistance. During sliding action, the fused coatings exhibit tribo-oxide layers, which provide the best wear resistance of the microwave fused composite coatings. The wear resistance of the WC12Co coatings is improved as compared to CeO_2 modified WC12Co coatings.

Keywords: HVOF, WC12Co, Microwave fused, As-sprayed, Sliding wear, Microhardness

1 Introduction

Most of the mechanical industries, such as aircraft, automobiles, defence, turbines, tools and die are seeking newer technologies to restore and improve surface properties as technology advances. Materials used in these mentioned applications undergo critical degradations, such as failure due to corrosion, erosion and wear [1]. The coating is one of the solutions to avoid surface degradation and to preserve the base alloy properties in harsh environments [2]. Nevertheless, alloy production alone cannot get all the essential mechanical properties [3]. An alternative approach, in which mechanical strength is achieved through alloy production and wear or oxidation resistance is provided through surface reform using various coating techniques, is a commonly accepted practice in early state applications [4]. Compared to conventional thermal spray techniques, the HVOF (High Velocity Oxygen Fuel) technique produces a thick and hard covering with less porosity. HVOF coatings are widely used to control abrasive, adhesive, and erosive wear in high-temperature applications. To solve the industrial difficulties connected with component material,

HVOF technology is the most appropriate technique for coating the alloys [5], [6]. Meanwhile, even with cutting-edge coating technology, it is impossible to create defect-free thermal spray coatings. Whenever the HVOF process is carried out in the presence of air, it is very easy for air to become trapped in the coating zone. This can result in deficiencies such as voids and pores, which arise from the spraying process and are present at the splat borders, where the coatings are primarily impacted by wear and corrosion [7], [8]. However, it is not possible to achieve defect-free thermal spray coatings using state-of-the-art technology for coating systems [9], [10]. Usually, residual stresses are present in the HVOF process due to the drastic velocity of the liquid particles. In order to reduce residual stress, the thermal spray coating must be carried out in the vacuum region, but this kind of coating production is highly expensive. It can be accomplished by various post-treatment processes, such as conventional furnace treatment, laser and electron beam treatment, etc. [11]. However, there are a few downsides to the laser and electron beam processes, such as expensive processing and maintenance costs. Furthermore, because of the quick cooling rate, there is a higher risk of crack propagation during solidification and significant thermal deformation of the base material. Whereas traditional heat-treating procedures are less expensive but take longer time to process [12]. Microwave post-treatment is now the most used method for improving the characteristics of thermal coatings. There are only a few studies on the microwave post-treatment procedure. There is a limited amount of literature available on the variables that influence microwave fused thermal coatings and the induction of carbon in the coatings to produce carbides and to improve wear resistance [13], [14].

In this study, WC-12Co and CeO_2 powder and AISI4140 steel alloy are selected as coating composition and base metal respectively. The 10 to 50 μm sized coating powder was crushed using the high energy ball milling method. The feedstock was then sprayed over the base alloy using the HVOF spray technique, followed by microwave fusion. Mechanical and microstructural properties of WC-12Co and WC-12Co+4% CeO_2 coatings have been investigated before and after microwave treatment. Sliding wear tests were also performed at various temperatures and loads in dry conditions. The wear rate was determined using the volume loss of the substrate and coatings separately. Finally, with SEM, XRD and EDS techniques, the material loss by wear test was investigated.

2 Materials and Methods

2.1 *Materials*

Commercially available pure AISI4140 steel alloy substrate with dimensions of 100 × 100 mm pieces was acquired from New Arise Metal Ltd., Maharashtra, India. The feedstock WC-12Co (WC104) and CeO_2 (NS6130-05-546) are obtained from JD Powder Metallurgy in Andhra Pradesh, India, in size ranges between 10–50 μm. In a high-intensity ball milling process lasting about 2 h, 4% Cerium Oxide (CeO_2) is added with 96% Tungsten Carbide and cobalt (WC-12Co) under inert conditions. Tungsten carbide balls with the size of 12 to 18 mm. Ball milling was done at dry condition and powder weight was 100 g. The milling conditions used for the processing of WC12Co (96%) + CeO_2 (4%) feedstock (weight percentage) are reported in Table 1.

Table 1: High-intensity ball milling parameters

Method	HEBM Speed, rpm	Ball to Powder Weight Ratio	Weight, g	HEBM Time, h
HIBM	250	8:1	100	2

2.2 *Coating development*

The milled feedstock is coated on the substrate at Aum Techno Spray Pvt. Ltd. in Bangalore, India, using a Hipojet-2100 diamond jet gun HVOF apparatus. Before coating, the upper layer of the substrate was roughened using alumina grit blasting and then cleaned with acetone to improve adhesion between the substrate surface and the coating. The substrate temperature is monitored using a thermocouple throughout spraying and is kept at 180 °C. Table 2 lists the HVOF thermal spray process variables.

To enhance coating adherence, the whole spray process is kept at a higher fuel flow while lowering the powder feed rate and standoff distance, according to several studies. The main causes above are due to its large impact on particle velocity, and a decrease in powder feed rate that leads to a considerable rise in particle velocity and increases compressive residual stress. The greater particle velocity also aids in

the smoothing of splats in coatings, which leads to enhanced splat adherence [15], [16].

Table 2: HVOF thermal Spray process variables

Variables	Value
Fuel–Hydrogen	600 lpm
Carrier gas–Nitrogen (N_2)	42 lpm
Air	200 lpm
Powder feed rate	18 g min^{-1}
Combustion pressure	10 bar
Spray distance	250 mm
Thickness	200 microns
Angle between gun to job	90º
Traverse velocity	80 m/min

2.3 *Microwave re-melting of deposition*

After the WC12Co-CeO_2 feedstock was deposited, the specimens were cut into 10 × 10 × 5 mm pieces using wire EDM equipment for domestic microwave treatment. Figure 1 describes the microwave fusing operating principle. Initially, the sprayed samples were properly placed on the refractory brick, and a 1 mm thick pure graphite sheet was persistently placed above them to induce carbon in the fusing process. After being placed, the as-sprayed coating samples are covered with a refractory block to prevent heat loss [17], [18]. Microwaves are captured by a silicon carbide (SiC) susceptor, which is positioned over the graphite sheet, and heat is transmitted to the as-sprayed coating, resulting in the re-melting process. After completing the setup, a power of 950 W with a frequency range of 2.5 GHz is supplied for the duration of the 12 min fusing process for the as-sprayed coating. After finishing the re-melting process, the samples were gradually allowed to cool to ambient temperature.

2.4 *Characterization of as-sprayed and microwave fused coatings*

The coating sample's microstructure was examined in cross-section. EDM equipment was used to cut specimens along the cross-section. The samples were polished using SiC paper ranging from 600 to 2000 grit, and the ultimate polishing was made with velvet cloth and superfine diamond paste. SEM was used to evaluate surface and cross-sectional microstructures, while EDS was used to analyze chemical composition.

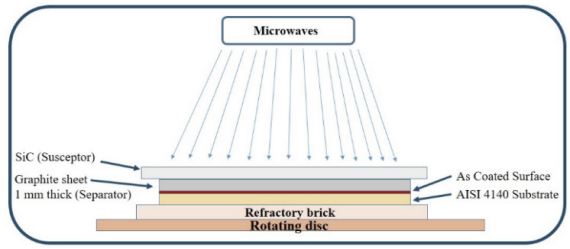

Figure 1: Microwave processing.

X-ray diffraction was used to identify the existence of intermetallic recrystallization phases as well as other phases, such as oxides and carbides in as-sprayed and microwave-treated coatings.

2.5 *Microhardness and dry sliding wear test*

Vickers microhardness (Chemical & Metallurgical Labs Pvt. Ltd. Banglore) was determined along the smoothed cross-section of the as-sprayed and fused coating at 300 g load for 30 s dwell time. The mean value of microhardness was recorded by taking eight indentations at different locations. The dry sliding wear performance of as-sprayed and microwave fused coatings was investigated using a pin-on-disk apparatus in an unlubricated environment in accordance with the ASTM G99-05 standard. The wear tests were carried out under loading conditions of 20 and 40 N at 1.4 m/s over a continuous sliding distance of 3200 m for both as-sprayed and microwave fused coatings. The experiments were performed at three different temperatures: room temperature, 200, 400, and 600 °C. The pin heating system was utilized to maintain the appropriate temperature.

The interacting surfaces were sanded with 1200 mesh sandpaper, then washed with acetone and dried. The instrument was outfitted with a sample heating facility, and a thermocouple was employed to test the pre-set temperature. After the test, raw data was obtained to analyze the volume loss, friction coefficient and wear rate based on the sample's height loss.

3 Results and Discussion

3.1 *WC12Co and WC12Co+CeO_2 feedstock morphologies*

Figure 2(a) and (b) depict the microstructural

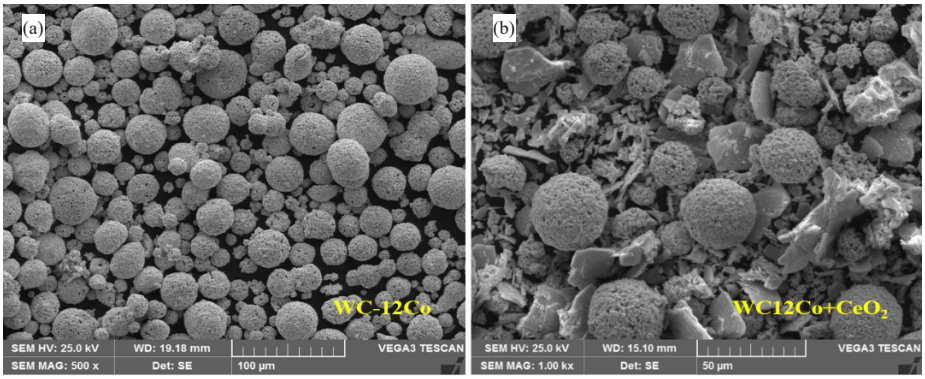

Figure 2: (a) Morphology of WC12Co and (b) WC12Co+CeO_2 compositions.

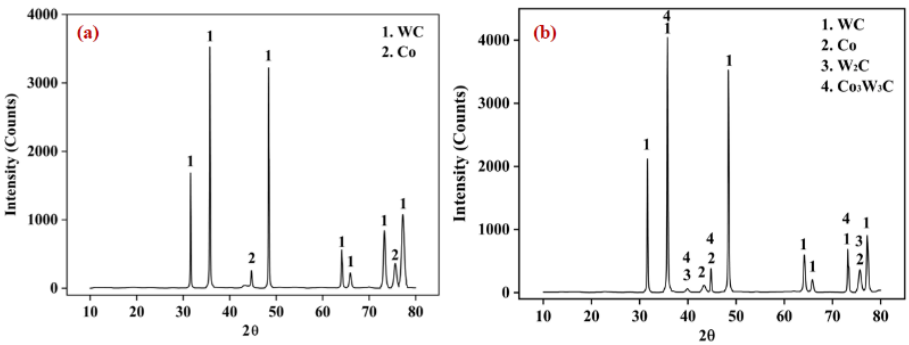

Figure 3: XRD pattern of (a) as-coated and (b) microwave fused WC12Co composition.

characteristics of WC12Co and WC12Co+CeO_2 feedstock before deposition. The WC12Co feedstock was produced by sintering and has a spherical form with the size ranging from ranges between 10–50 µm. CeO_2 feedstock is also synthesised using the same process and it is cubic fluorite-type in fcc structure [19]. The cross-sectional morphologies of WC–12Co powders show that moderately dense WC particles are well bound with the cobalt structure.

3.2 *Phase and coating structure analysis*

Figure 3(a) and (b) shows the XRD analysis of as coated WC12Co and microwave fused WC12Co depositions, respectively. In the XRD examination, basic carbides, such as WC and Co were observed in the peak of as-coated deposition. Whereas it was observed that WC dissolution resulted information of W2Cand WC, as well as recrystallization of amorphous binder to Co3W3C, with their stability rising with increasing heat treatment temperature.

During the microwave process, carbon was driven into the coating out from the graphite sheet, resulting in the formation of a new rich tungsten carbide W2C. The metastable Co3W3C phase lacked a consistent crystalline structure and was riddled with flaws. As previously stated, the cobalt in the coating interacts with tungsten carbides to create the elementary tungsten. This might be attributable to the molten pool's different phase constituents and complex temperature distribution [20], [21]. Furthermore, as coated WC12Co+CeO_2 and microwave fused WC12Co+CeO_2 deposition is shown in the Figures 4(a) and (b). The powder is made up of three phases: WC, Co, and CeO_2. The peak of the as-sprayed coating comprises a minor amount of Co and CeO_2 phases, but the coating is mainly composed of the WC phase. In post-treatment deposition, the chemical interaction between CeO_2 and Ce atoms, as well as the partial breakdown of $CeCO_2$/Ce5Co19 were detected. When the microwave process is performed under open circumstances, certain oxide phases are developed,

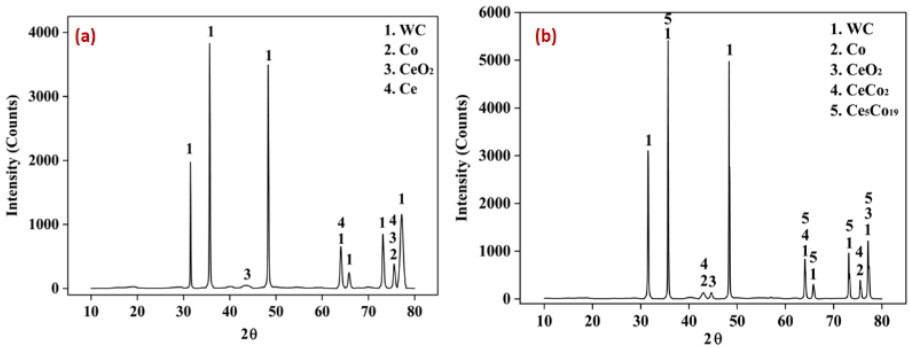

Figure 4: XRD pattern of (a) as-coated and (b) microwave fused WC12Co+CeO_2 composition.

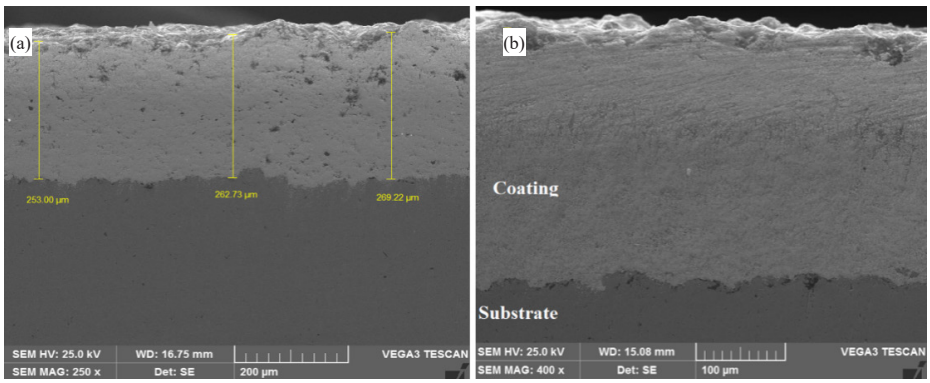

Figure 5: (a) Morphology of as-coated and (b) microwave fused coatings C/S.

which leads to the microstructure of the coatings being strengthened [22].

Figure 5(a) and (b) of SEM micrographs of as-sprayed and microwave-treated coatings along a cross-section demonstrate a laminar and homogenous structure that is well bonded to the substrate. Both compositions achieve an average coating thickness of around 260 µm and a surface roughness of 6.53 µm. In comparison, the as-sprayed coating exhibits significant cracking and voiding, as seen by morphology. Also, microwave fused deposition improves metallurgical bonding by allowing components to diffuse through the contact between the coating and the base metal. The roughness value is 6.53 and 3.43 µm for WC-Co coating for as-sprayed and microwave samples, respectively. Whereas, for WC-Co+CeO_2 coating slight variation is observed i.e. 6.12 and 3.38 µm. The error range is ±0.62 and ±0.94. The microwave remelts the partially melted and unmelted elements with the duration of 12 min for both the compositions as shown in Figures 5(a) and (b) and Figures 6(a) and (b).

The microwave fused coating has a minimal numbers of unmelted particles and a homogeneous structure. The greater amount of pores, microcracks, cavities and lamellar structures were removed from the as-coated samples. Figure 7(a) depicts a micrograph of the as-sprayed coating across a cross-section, revealing a laminar and homogeneous structure that is well bound to the substrate. The morphology of the as-sprayed coating reveals cracks and cavities. Figure 7(b) revels, SEM micrograph of microwave fused coating cross-section reveals a homogenous structure with fewer defects in the fused zone. The remelted deposition exhibits good metallurgical bonding due to element inter-diffusion across the coating-substrate interface.

Figure 8(a) and (b) describes the EDS analysis of the as-coated and microwave fused WC12Co coatings, respectively. According to the EDS result, there is not much of an increase in oxides, but the percentage of carbon particles is higher due to the influence of post-treatment. This results in a harder surface than the

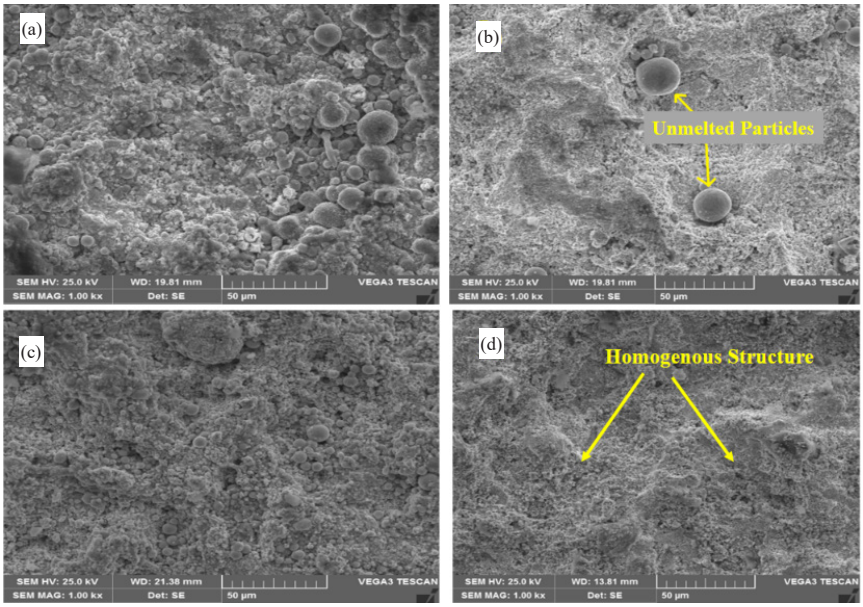

Figure 6: Morphology of (a) as-coated WC12Co and (b) microwave fused WC12Co Compositions, (c) as-coated WC12Co+CeO_2 and (d) microwave fused WC12Co+CeO_2 Compositions.

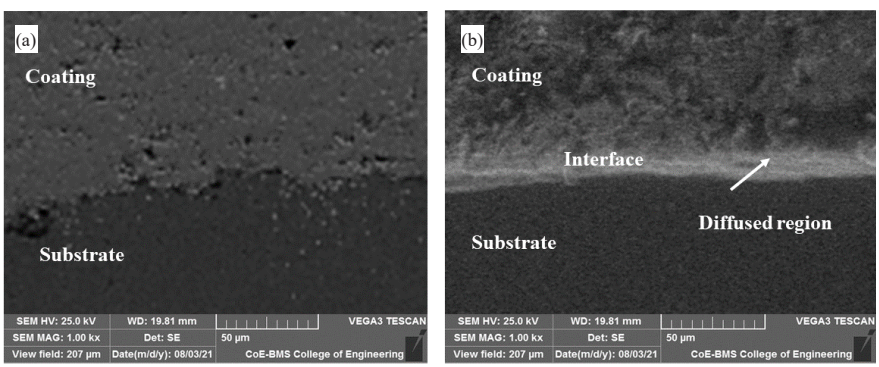

Figure 7: Micrographs along the cross-section of WC12Co coatings (a) as-sprayed (b) microwave fused.

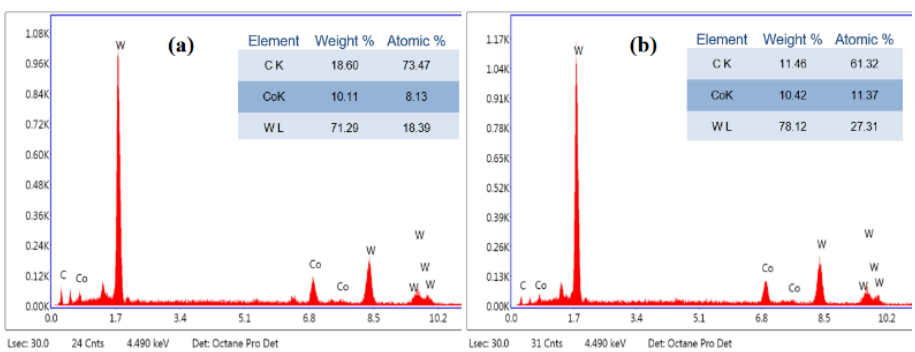

Figure 8: EDS analysis of (a) microwave fused WC12Co and (b) as-coated WC12Co coatings.

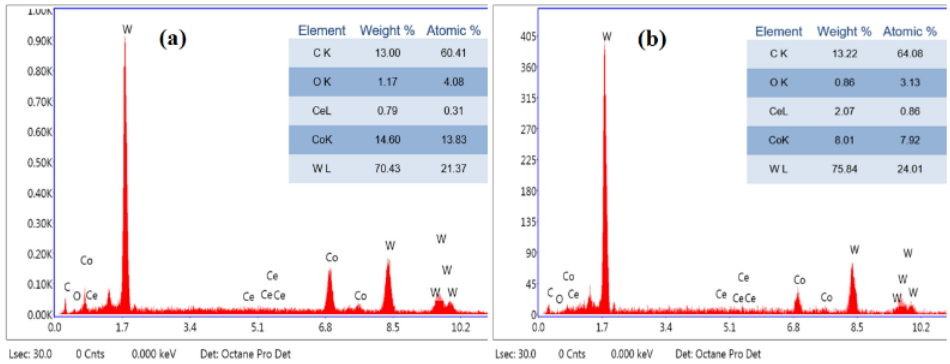

Figure 9: EDS analysis of (a) as-coated WC12Co+CeO_2 and (b) microwave fused WC12Co+CeO_2 coatings.

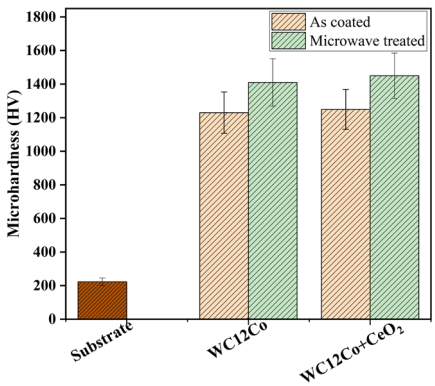

Figure 10: Microhardness with a load of 300 g.

as-sprayed coating surface. The results indicate that the oxide percentage of coating materials is distributed equally. Similarly, Figures 9(a) and (b) depict the EDS analysis of the as-coated and microwave fused WC12Co+CeO_2 coated compositions, respectively. As discussed earlier, the percentage of carbon increases in microwave fused coatings leads to the harder microstructure of the coating.

The difference in microhardness evaluated from various coatings with a load of 300 g at the coating is depicted in Figure 10. The average microhardness of as-sprayed and microwave fused WC12Co coatings are 1230 ± 35 and 1410 ± 60HV, respectively. Similarly, 1250 ± 40 and 1450 ± 65 HV were found from as-sprayed and microwave fused WC12Co+CeO_2 coatings, respectively. Since the compositions are compared, the base metal has a lower microhardness value of about 223 ± 25 HV. Because of metallurgical bonding generated by inter diffusion of particles, the microhardness of the substrate-coating interface of fused coatings is improved. However, the quick solidification that occurs during the microwave heat treatment results in strengthened grains. Furthermore, the hard phases of WC12Co+CeO_2 can increase the hardness of the microwave fused coating [23].

3.3 *Dry sliding wear performance*

The dry sliding wear behavior of WC12Co and WC12Co+CeO_2 compositions were investigated both as coated and microwave fused coatings. Wear loss and friction coefficient are two main parameters that are taken into consideration during the wear test to determine the coatings' wear rate. In the dry sliding wear test, WC12Co and WC12Co+CeO_2 compositions, the microwave-fused coatings exhibited lower friction and higher wear resistance than the as-sprayed coating under loads of 20 and 40 N at various temperatures. This was owing to the increased hardness and metallurgical bonding between the substrate and the coating during the microwave heat treatment. Figure 11 depicts the wear rate of the two composite coatings for a 20 N load at various temperatures. The wear rates increased as the test temperatures and applied load increased. The wear rate of as-sprayed deposition is about three times that of microwave fused coatings as shown the Figure 11. Figure 12 exhibits the wear rate of both compositions at a standard load of 40 N at various test temperatures for as-coated and microwave fused coatings. Even in the 40 N load condition, the as-sprayed coating wear rate is three times greater than the microwave fused coatings. Both coated compositions had a high wear rate at 600 °C under loads of 20 and 40 N, as shown in Figures 11 and 12. Figures 13 and 14

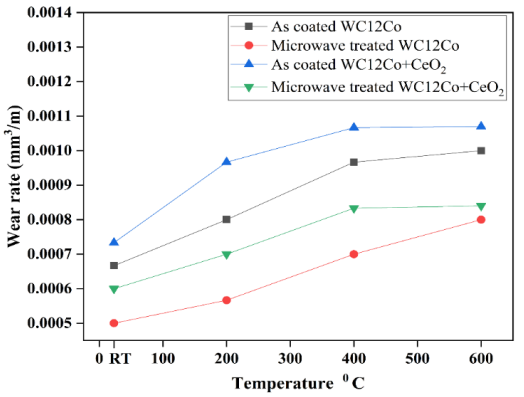

Figure 11: Wear rate of as-coated and microwave fused coatings for 20 N load.

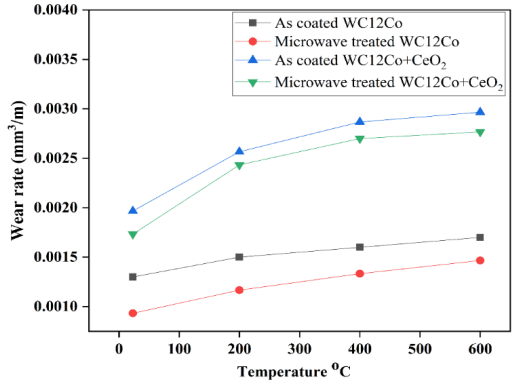

Figure 12: Wear rate of as-coated and microwave fused coatings for 40 N load.

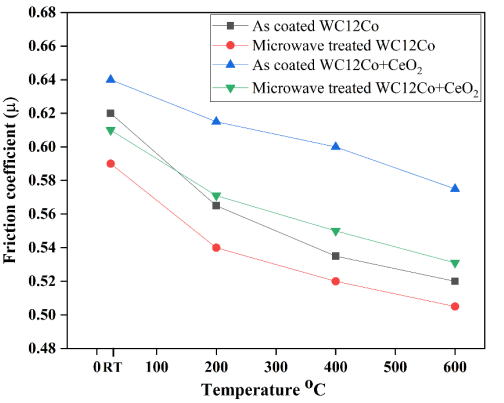

Figure 13: Friction coefficient of as coated and microwave fused coatings for 20 N load.

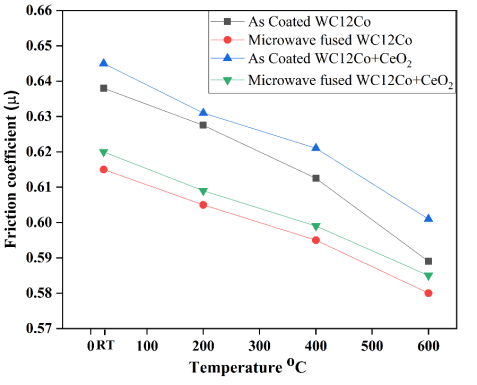

Figure 14: Friction coefficient of as-coated and microwave fused coatings for 40 N load.

demonstrate the friction coefficient of as-sprayed and microwave fused coatings for the load of 20 and 40 N, respectively. Figures 14 and 15 illustrate the average value of the friction coefficient, which is recorded for each test. Typical friction coefficient values for as-sprayed coatings are significantly greater than values for fused coatings assessed at high temperatures. Rapid material loss due to adhesion phenomena and a rise in flash temperature are the causes of an increase in friction coefficient in as-sprayed coatings. Furthermore, as observed in Figures 11 and 12, the unmodified CeO_2 coatings have the lowest abrasive wear in both the as-sprayed and microwave fused coatings.

As discussed in several research articles, the addition of CeO_2 more than 2 wt% does not improve the wear resistance of the coatings [24]–[27]. A modified composition comprising less than 2% wt. CeO_2 offers the greater wear resistance, according to many authors. However, in this work, the WC12Co coating is modified with 4 wt% CeO_2, and the wear rate is significantly increased when compared to the unmodified WC12Co coating. Excessive rare earth elements will accelerate the breakdown of WC and Co particles, and the hardness and wear resistance of the cladding layer will be reduced when a considerable number of WC and Co particles are burnt away. As a result, in the wear test, the shield layer causes significant plastic distortion, and the reinvest is wide and deep [28], [29].

3.4 *Surface morphologies of worn surfaces as evaluated by SEM*

The worn surface morphologies of WC12Co as-sprayed and microwave fused coatings with varying

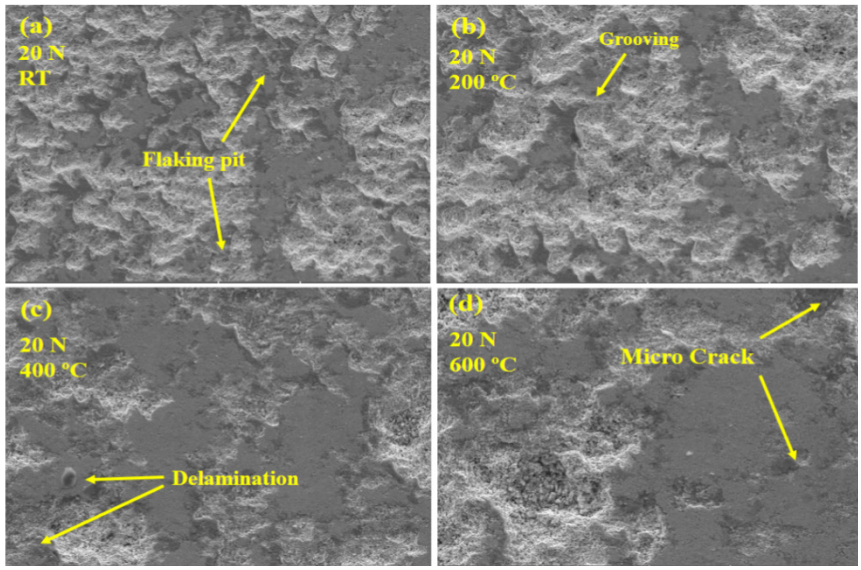

Figure 15: Worn surface SEM analysis of as-sprayed WC12Co coating under 20 N load.

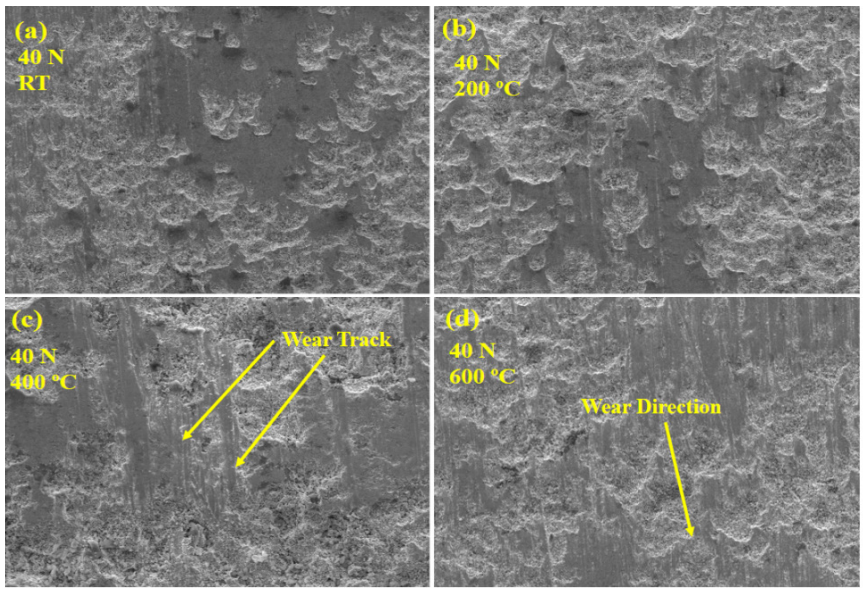

Figure 16: Worn surface SEM analysis of as-sprayed WC12Co coating under 40 N load.

load and temperature are depicted in Figures 15 and 16. The worn surfaces of as-sprayed WC12Co coatings under 20 and 40 N normal loads are characterized by fissures, rupture and splat separation as presented in Figures 15 and 16 respectively. As the typical load is increased to 40 N, the wear of the as-sprayed coating is impacted by intersplat cohesion, as shown in Figure 16(a)–(d). At high temperatures and loads, the wear scar is harsh and the track width increases. Whereas, Figures 17 and 18 indicate the morphology of the microwave fused wear surface of the WC12Co composition. Remelting promotes intersplat cohesiveness in microwave fused coatings, resulting in reduced material loss. Figures 17 and 18 show that at 20 N normal load, the worn surface is smooth in various regions, tiny bits of coating materials are

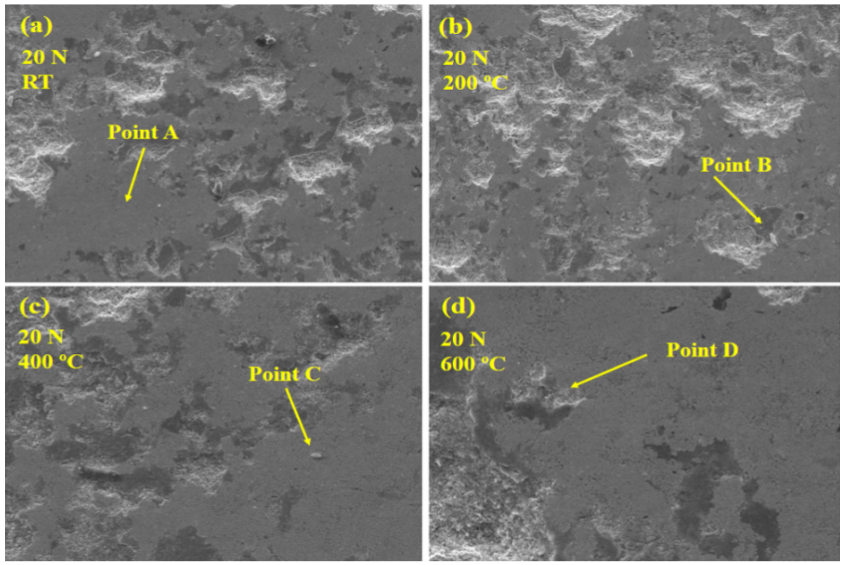

Figure 17: Worn surface SEM analysis of microwave fused WC12Co coating under 20 N load.

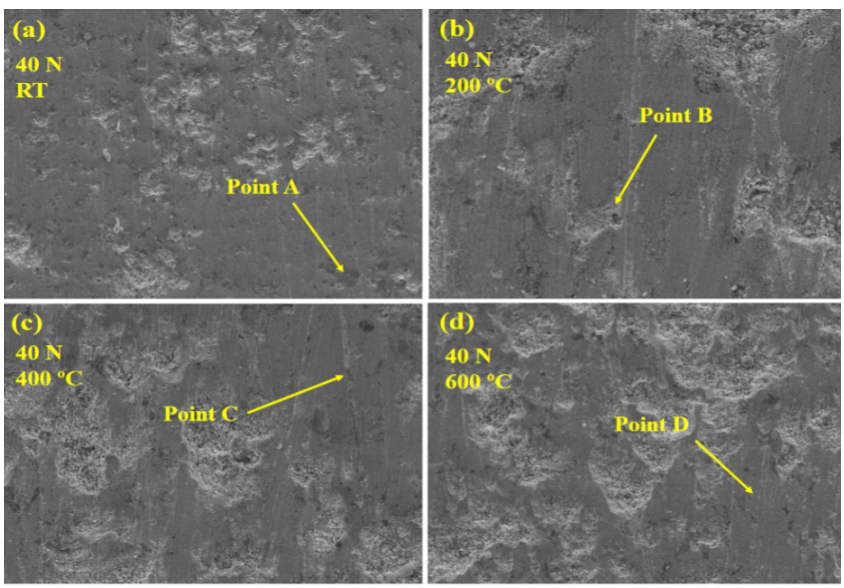

Figure 18: Worn surface SEM analysis of microwave fused WC12Co coating under 40 N load.

pushed away, and small peeling pits can be seen on worn surfaces. Due to the microwave effect, the presence of supplementary carbide, such as W2C provides an extremely hard surface, resulting in fatigue cracking at 200, 400, and 600 °C screening temperatures.

At high temperatures, the protective oxide coatings that form lack adequate sliding motion, causing the oxide film to fracture. This led to an increase in wear rate and volume loss as the temperature increased. The influence of temperature revealed that at high temperatures of 400 and 600 °C, the wear resistance of as-coated samples was considerably condensed for both compositions. The mass strength of most metallic materials diminishes when exposed to high temperatures.

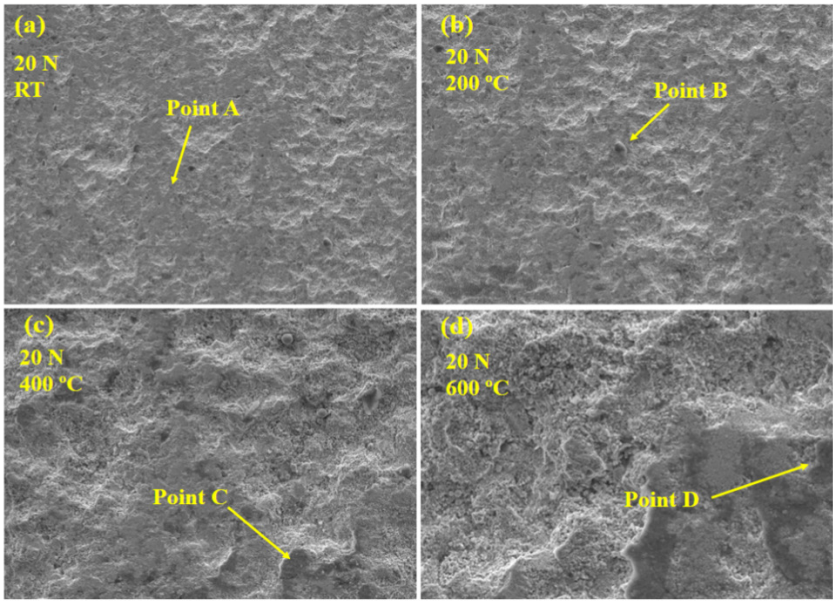

Figure 19: Worn surface SEM analysis of as sprayedCeO_2 added WC12Co coating under 20 N load.

Due to its lower hardness, this contributed to the increased wear rate at high temperatures [30]. Even when the applied stress was raised, there was a constant rupture of the protective oxidation layer (Figures 15 and 16), which allowed for greater metallic contact and adhesion, resulting in a faster wear rate. Microwave fused coatings have a lower wear rate than as-sprayed coatings. This demonstrated that the microwave heating technique minimized material loss during sliding action by increasing coating hardness and refining the microstructure without the existence of cracks (Figures 17 and 18).

Microwave fused coatings had lower friction coefficients at increased temperatures of 400 °C and 600 °C than at a lesser temperature of 200 °C. In fused coatings, the quick oxidation reaction causes an increase in friction at first, but the friction trend remains constant over time, when compared to the coarser oxidized regions created by as-sprayed coatings. This implies that oxidized regions on the coating wear scar are finer and more frequent. However, it reduces adhesive wear and prevents the rise in recurrent periodic friction caused by the quick accumulation of oxides [4]. Also noted throughout the sliding movement is the tremendous loss of coating material produced by pulling out of optimal splats, implying severe wear. This might be because of the existence of partially melted cobalt and tungsten particles [31]. As the flicker temperature rises, an oxide layer of coating active components forms in between the coating and the corresponding surface. This prevents additional coating material loss at the greater loads, resulting in the lesser wear loss [32].

The wear mechanism has been altered from adhesive to tribo-oxidative, since during high temperature wear condition simultaneous material loss by wear and oxidation takes place. Figures 17 and 18 show morphologies that are similar to those found for the 40 N normal load test condition. Figures 17 and 18 illustrate similar morphologies produced for a 40 N normal load test, as well as some propagation of cracks and fatigue spelling wear mechanisms. As test temperatures rise, a rapid oxidation layer forms, and this layer grows larger in 40 N normal load testing. Higher oxide levels are related to lower wear and friction.

Although the oxide production is anticipated to aid in friction stabilization (because of the lower chemical coherence of the surfaces and the oxides' self-lubricating capabilities), the weak oxide adherence to the coated surface remains enables adhesive wear. Wear traces were seen at evaluated temperatures during high load, say 40 N test circumstances. The worn morphology of CeO_2 modified WC12Co coating is depicted in Figures 19–22

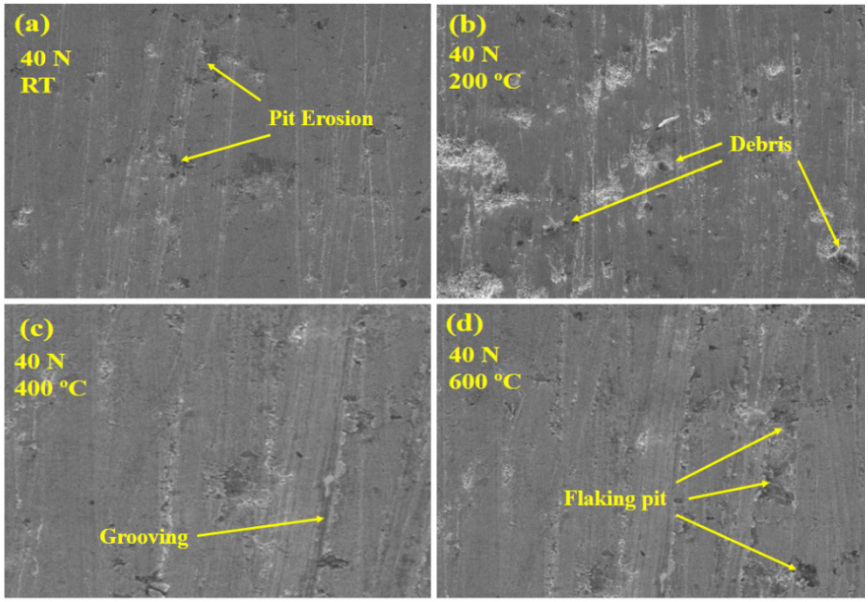

Figure 20: Worn surface SEM analysis of as sprayedCeO_2 added WC12Co coating under 40 N load.

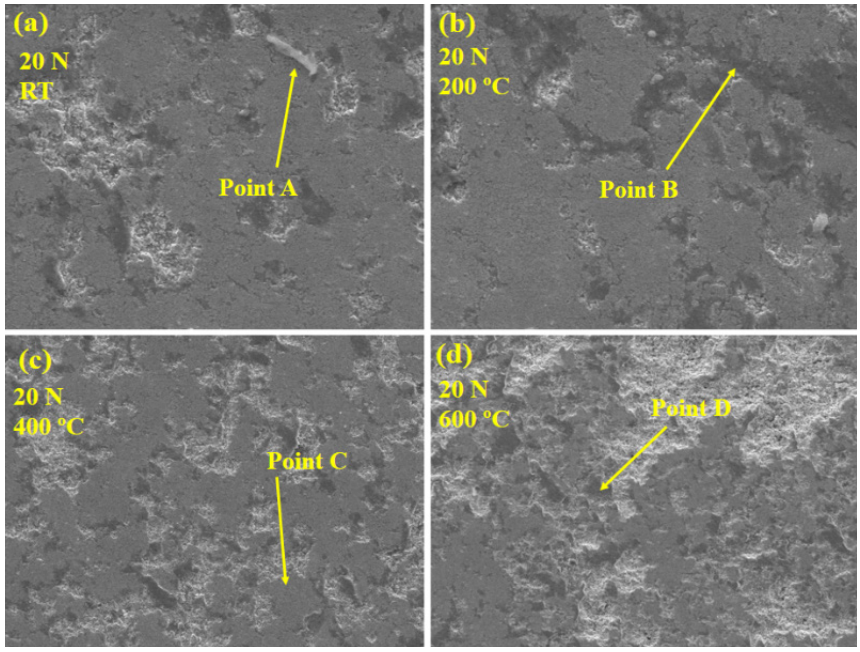

Figure 21: Worn surface SEM analysis of microwave fused CeO_2 added WC12Co coating under 20 N load.

for both as-sprayed and microwave fused coatings performed at varied load and testing temperatures. Under typical loads of 20 and 40 N, the worn surfaces (Figures 19 and 20) of as-sprayed CeO_2 modified coating are characterized by grooving, rupture, flaking pit, and so on. Wear loss occurs with increasing load and temperature, and is associated with cracking, grooving, and wear track width. Whereas in microwave fused CeO_2 modified coating, as presented in Figures 21 and 22, at normal loads of 20 and 40 N,

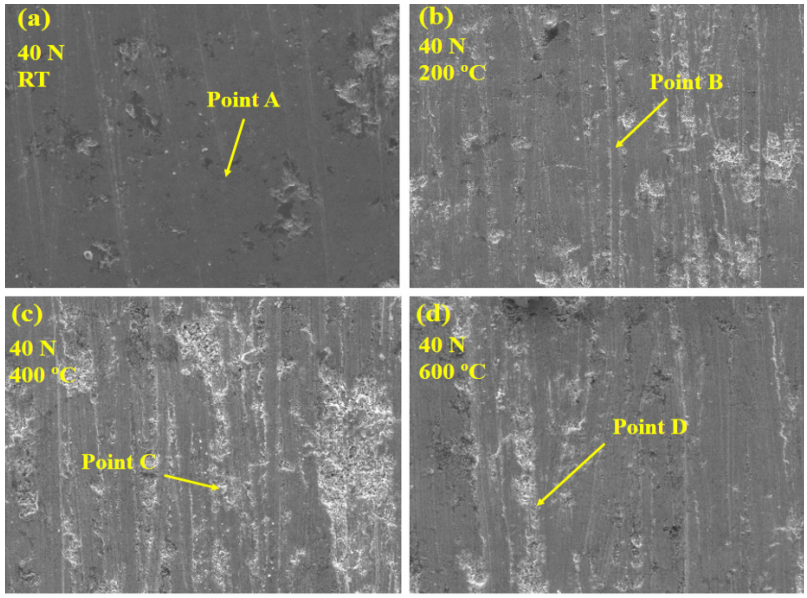

Figure 22: worn surface SEM analysis of microwave fused CeO_2 added WC12Co coating under 40 N load.

the worn surface is smooth in certain areas, very little coating material is driven away, and small peeling pits may be seen on worn surfaces. While WC12Co and CeO_2 modified WC12Co coating compositions were compared for both as-coated and microwave fused coatings, CeO_2 modified WC12Co coatings had increased wear loss. Because of the high rare earth concentration, the particle size rises in the cladding layer, resulting in a certain amount of reunion, as seen in Figures 20 to 22. The particles predominantly are comprising of the components WC, Co, C, and Ce and the Ce element is found in practically all sections of the fragments.

The excessive rare earth element in the coating restricts the precipitation of secondary WC and Co particles, as the initial WC and Co particles dissolved into W, Co and C components. To summarize, the proper rare earth can encourage the spheroidization and refining of the original WC and Co ceramic particles, resulting in a more homogenous distribution and a high number of secondary WC and Co ceramic particles precipitating from the matrix. Excessive rare earth causes severe burn loss in the original WC and Co molecules, and the second solubilized phases are constrained, resulting in the formation of WC/Co/C compounds. Again, the greater wear rate was reported in the as coated samples, even in the CeO_2 modified WC12 Co coatings. Without rare earth (CeO_2), the worn surface of the laminate structure has less wide and deep ploughed grooves, as well as some scattering phenomena, as seen in the rare earth modified coating in Figures 19 to 22.

4 Conclusions

The AISI 4140 steel alloy substrate was successfully deposited by WC12Co and CeO_2 modified WC12Co composition by HVOF technique. The coatings were consistent in homogeneous structure with an average thickness of 260 µm. The microwave post-heating method was used effectively to modify WC12Co and CeO_2 modified WC12Co coatings by improving metallurgical bonding and structure. A comparison of substrate, as-sprayed coatings, and microwave treated coatings revealed that microwave fused coatings for both WC12Co and CeO_2 modified WC12Co compositions had a high microhardness. The friction coefficient was reduced with increasing temperature in the as-sprayed and fused coatings for typical loads of 20 N and 40 N for both compositions. The fused covering produced various brittle phases at higher temperatures, including Ce5Co19, $CeCO_2$ and CoWC. At higher temperatures, these oxide phases acted as both solid and liquid lubricants. As compared

to as-sprayed coatings, the fused layer demonstrated a better wear function with greater width and smoother wear tracks, resulting in the greater wear resistance. Microwave heating post-treatment of coatings has been shown to be beneficial in enhancing the metallurgical and mechanical characteristics of as-sprayed coatings. After comparing all WC12Co and CeO_2 modified WC12Co compositions, the WC12Co coatings exhibited better wear resistance under varying load and temperature conditions.

References

[1] E. Bemporad, M. Sebastiani, F. Casadei, and F. Carassiti, "Modelling, production and characterisation of duplex coatings (HVOF and PVD) on Ti–6Al–4V substrate for specific mechanical applications," *Surface and Coatings Technology*, vol. 201, no. 18, pp. 7652–7662, Jun. 2007, doi: 10.1016/j.surfcoat.2007.02.041.

[2] T. Peat, A. M. Galloway, A. I. Toumpis, and D. Harvey, "Evaluation of the synergistic erosion-corrosion behaviour of HVOF thermal spray coatings," *Surface and Coatings Technology*, vol. 299, pp. 37–48, Aug. 2016, doi: 10.1016/j.surfcoat.2016.04.072.

[3] M. R. Ramesh, S. Prakash, S. K. Nath, P. K. Sapra, and B Venkataraman, "Solid particle erosion of HVOF sprayed WC-Co/NiCrFeSiB coatings," *Wear*, vol. 269, no. 3, pp. 197–205, Jun. 2010, doi: 10.1016/j.wear.2010.03.019.

[4] G. Bolelli and L. Lusvarghi, "Heat treatment effects on the tribological performance of HVOF sprayed Co-Mo-Cr-Si coatings," *Journal of Thermal Spray Technology*, vol. 15, no. 4, pp. 802–810, Dec. 2006, doi: 10.1361/105996306X146721.

[5] G. Y. Koga, R. Schulz, S. Savoie, A. R. Nascimento, Y. Drolet, C. Bolfarini, C. S. Kiminami, and W. J. Botta, "Microstructure and wear behavior of Fe-based amorphous HVOF coatings produced from commercial precursors," *Surface and Coatings Technology*, vol. 309, no. 15, pp. 938–944, Jan. 2017, doi: 10.1016/j.surfcoat.2016.10.057.

[6] D. G. Pradeep, C. V. Venkatesh, and H. S. Nithin, "Review on tribological and mechanical behavior in HVOF thermal-sprayed composite coatings," *Journal of Bio-and Tribo-Corrosion*, vol. 8, no. 1, pp. 1–9, Mar. 2022, doi: 10.1007/s40735-022-00631-x.

[7] J. A. Picas, M. Punset, S. Menargues, E. Martín, and M. T. Baile, "Microstructural and tribological studies of as-sprayed and heat-treated HVOF Cr_3C_2–CoNiCrAlY coatings with a CoNiCrAlY bond coat," *Surface and Coatings Technology*, vol. 268, no. 25, pp. 317–324, Apr. 2015, doi: 10.1016/j.surfcoat.2014.10.039.

[8] P. Potejana and N. Seemuang, "Fabrication of metallic nano pillar arrays on substrate by sputter coating and direct imprinting processes," *Applied Science and Engineering Progress*, vol. 14, no. 4, pp. 72–79, 2021, doi: 10.14416/j.asep.2019.09.001.

[9] P. Kongkaoroptham, M. Boonpensin, T. Siripongsakul, and P. Promdirek, "Corrosion behaviour of AISI409 stainless steel with Al slurry coating in molten salt," *Applied Science and Engineering Progress*, vol. 15, no. 1, 2022, Art. no. 3523, doi: 10.14416/j.asep.2021.02.002.

[10] P. Adisak, B. Sompong, Y. Trinet, and R. Aphichart, "Numerical modeling for corrosion rate between heat-affected zone and unaffected base metal of galvanized steel welded by Brazing," *Applied Science and Engineering Progress*, vol. 15, no. 3, 2022, Art. no. 4539, doi: 10.14416/j.asep.2021.03.001.

[11] Y. Wang, C. G. Li, W. Tian, and Y. Yang, "Laser surface remelting of plasma sprayed nanostructured Al_2O_3–13wt% TiO_2 coatings on titanium alloy," *Applied Surface Science*, vol. 255, no. 20, pp. 8603–8610, Jul. 2009, doi: 10.1016/j.apsusc.2009.06.033.

[12] M. Bhattacharya and T. Basak, "A review on the susceptor assisted microwave processing of materials," *Energy*, vol. 97, no. 15, pp. 306–338, Feb. 2016, doi: 10.1016/j.energy.2015.11.034.

[13] C. D. Prasad, S. Joladarashi, M. R. Ramesh, M. S. Srinath, and B. H. Channabasappa, "Influence of microwave hybrid heating on the sliding wear behaviour of HVOF sprayed CoMoCrSi coating," *Materials Research Express*, vol. 5, no. 8, Jul. 2018, Art. no. 086519, doi: 10.1088/2053-1591/aad44e.

[14] D. G. Pradeep, H. S. Nithin, B. N. Sharath, K. S. Madhu, and C. V. Venkatesh, "Microstructure and wear behavior of microwave treated WC-10Co-4Cr composite coating on AISI 4140 alloy steel," in *IOP Conference Series: Materials*

Science and Engineering, vol. 1189, no. 1, 2021, Art. no. 012012, doi: 10.1088/1757-899X/1189/1/012012.

[15] A. G. Pukasiewicz, H. E. De Boer, G. B. Sucharski, R. F. Vaz, and L. A. Procopiak, "The influence of HVOF spraying parameters on the microstructure, residual stress and cavitation resistance of FeMnCrSi coatings," *Surface and Coatings Technology*, vol. 327, no. 25, pp. 158–166, Oct. 2017, doi: 10.1016/j.surfcoat.2017.07.073.

[16] Q. Wang, Z. Chen, L. Li, and G. Yang, "The parameters optimization and abrasion wear mechanism of liquid fuel HVOF sprayed bimodal WC–12Co coating," *Surface and Coatings Technology*, vol. 206, no. 15, pp. 2233–2241, Jan. 2012, doi: 10.1016/j.surfcoat.2011.09.071.

[17] M. S. Lingappa, M. S. Srinath, and H. J. Amarendra, "Microstructural and mechanical investigation of aluminium alloy (Al 1050) melted by microwave hybrid heating," *Materials Research Express*, vol. 4, no. 7, Jul. 2017, Art. no. 076504, doi: 10.1088/2053-1591/aa7aaf.

[18] R. R. Mishra and A. K. Sharma, "On mechanism of in-situ microwave casting of aluminium alloy 7039 and cast microstructure," *Materials & Design*, vol. 112, no. 15, pp. 97–106, Dec. 2016, doi: 10.1016/j.matdes.2016.09.041.

[19] H. Ye, X. B. Zhang, Z. F. Xue, Y H Fan, and K Chen, "Effect of CeO_2 on microstructure and properties of WC/Ni60 coating by laser cladding," *Advanced Materials Research*, vol. 79, pp. 795–798, 2009, doi: 10.4028/www.scientific.net/AMR.79-82.795.

[20] D. A. Stewart, P. H. Shipway, and D. G. McCartney, "Influence of heat treatment on the abrasive wear behaviour of HVOF sprayed WC–Co coatings," *Surface and Coatings Technology*, vol. 105, no. 1, pp. 13–24, Jun. 1998, doi: 10.1016/S0257-8972(98)00444-7.

[21] J. Nerz, B. Kushner, and A. Rotolico, "Microstructural evaluation of tungsten carbide-cobalt coatings," *Journal of Thermal Spray Technology*, vol. 1, no. 2, pp. 147–152, Jun. 1992, doi: 10.1007/BF02659015.

[22] S. Sharma, "Abrasive wear study of rare earth modified coatings by statistical method," *Journal of Thermal Spray Technology*, vol. 21, no. 5, pp. 773–781, Sep. 2012, doi: 10.1007/s11666-012-9784-8.

[23] X. Qi and S. Zhu, "Effect of CeO_2 addition on thermal shock resistance of WC–12% Co coating deposited on ductile iron by electric contact surface strengthening," *Applied Surface Science*, vol. 349, no. 15, pp. 792–797, Sep. 2015, doi: 10.1016/j.apsusc.2015.05.064.

[24] S. Sharma, "Effect of CeO_2 addition on wear behavior of flame sprayed coatings," *Journal of Engineering & Technology*, vol. 4, no. 2, Jul. 2014, Art. no. 141.

[25] S. P. Sharma, D. K. Dwivedi, and P. K. Jain, "Effect of CeO_2 addition on the microstructure, hardness, and abrasive wear behaviour of flame-sprayed Ni-based coatings," *Proceedings of the Institution of Mechanical Engineers, Part J: Journal of Engineering Tribology*, Jul. 2008, vol. 222, no. 7, pp. 925–933, doi: 10.1243/13506501JET432.

[26] K. Singh and S. Sharma, "Development of Ni-based and CeO_2-modified coatings by microwave heating," *Materials and Manufacturing Processes*, vol. 33, no. 1, pp. 50–57, 2018, doi: 10.1080/10426914.2016.1257860.

[27] M. Li, S. Zhang, H. Li, Y. He, J. H. Yoon, and T. Y. Cho. "Effect of nano-CeO_2 on cobalt-based alloy laser coatings," *Journal of Materials Processing Technology*, vol. 202, no. 1, pp. 107–111, Jun. 2008, doi: 10.1016/j.jmatprotec.2007.08.050.

[28] Y. Cai, Z. Luo, Y. Chen, and S. Ao, "Influence of CeO_2 on tribological behaviour of TiC/Fe-based composite coating," *Surface Engineering*, vol. 12, no. 3, pp. 936–943, Dec. 2017, doi: 10.1080/02670844.2017.1309742.

[29] Y. Chen, Y. J. Chao, Z. Luo, Y. Cai, and C. Ma, "Microstructure and wear resistance of Co-based/Cr_3C_2 coatings with CeO_2," *Surface Engineering*, vol. 34, no. 8, pp. 588–595, Aug. 2018, doi: 10.1080/02670844.2017.1363484.

[30] G. Bolelli, L. M. Berger, M. Bonetti, and L. Lusvarghi, "Comparative study of the dry sliding wear behaviour of HVOF-sprayed WC–(W, Cr) 2C–Ni and WC–CoCr hardmetal coatings," *Wear*, vol. 309, no. 2, pp. 96–111, Jan. 2014, doi: 10.1016/j.wear.2013.11.001.

[31] H. L. Yu, W. Zhang, H. M. Wang, Y. L. Yin, X. C. Ji, and K. B. Zhou, "Comparison of surface

and cross-sectional micro-nano mechanical properties of flame sprayed NiCrBSi coating," *Journal of Alloys and Compounds*, vol. 672, no. 5, pp. 137–146, Jul. 2016, doi: 10.1016/j.jallcom.2016.02.118.

[32] R. Gonzalez, M. Cadenas, R. Fernandez, J. L. Cortizo, and E, "Rodríguez wear behaviour of flame sprayed NiCrBSi coating remelted by flame or by laser," *Wear*, vol. 262, no. 3, pp. 301–307, Feb. 2007, doi: 10.1016/j.wear.2006.05.009.